Fault-perpendicular aftershock clusters following the 2003 Mw = 5.0 Big Bear, California, earthquake

Wu-Cheng Chi[1,2] and Egill Hauksson[3]

Received 9 November 2005; revised 9 February 2006; accepted 14 February 2006; published 1 April 2006.

[1] To explore aftershock-triggering mechanisms for the 2003 Big Bear, California earthquake sequence, we determined differential travel-times and applied the double-difference technique to relocate these events, which formed three clusters. The main cluster coincides with the 3 km long northwest striking sub-vertical mainshock fault. The other two sub-vertical clusters, located at opposite ends of the mainshock rupture, are almost perpendicular to the mainshock fault, contradicting the 60° separation angle of conjugate faults as predicted from frictional laws. Allowing for a 30° uncertainty in the cataloged strike, dip and rake values about 75% of the aftershocks are strike-slip as determined from first motion and complete waveform moment tensor inversions. We use a mainshock conceptual slip model to derive Coulomb Failure Stress regions, and assess correlations between stress increases and aftershock locations. We conclude that the perpendicular aftershock clusters were triggered by the mainshock static stress perturbation. **Citation:** Chi, W.-C., and E. Hauksson (2006), Fault-perpendicular aftershock clusters following the 2003 Mw = 5.0 Big Bear, California, earthquake, *Geophys. Res. Lett.*, *33*, L07301, doi:10.1029/2005GL025033.

1. Introduction

[2] Laboratory uniaxial compressive tests of rock samples show 60° conjugate faults [e.g., *Twiss and Moores*, 1992]. In contrast, scientists often observe strike-slip faults intersecting each other at right angles (e.g., many examples by *Kilb and Rubin* [2002]). Several mechanisms have been proposed to explain the kinematics and mechanics of the orthogonal strike-slip faults and the accompanying seismicity. For example, *Kilb and Rubin* [2002] propose that perpendicular faults can be generated between two master strike-slip faults, in a style similar to the bookshelf block rotation. Low frictional properties of the faults can also increase the conjugate angles [e.g., *Townend and Zoback*, 2001].

[3] Here we explore if other mechanisms can also generate perpendicular seismicity. We use double-difference technique with differential travel-times to relocate the 2003 Big Bear, California mainshock (Mw = 5.0; Feb. 22, 2003; located at 116.847°W, 34.309°N, depth: 5 km) and its aftershocks (Figure 1). We systematically invert for focal mechanisms of this earthquake sequence. We construct a conceptual mainshock slip model to calculate Coulomb Failure Stress (CFS) pattern and correlate the CFS with the relocated aftershock hypocenters. Because of the difficulty to invert for aftershock locations and source parameters of small mainshock, only larger (Mw > 6) mainshock-induced CFS changes have been previously correlated statistically with the aftershock distribution [e.g., *Toda et al.*, 2002].

2. Double-Difference Relocations

[4] We relocated the Big Bear sequence using the double-difference technique of *Waldhauser and Ellsworth* [2000] based on the travel-time picks from the Southern California Seismic Network (SCSN) and differential travel times determined with waveform cross correlation [*Hauksson and Shearer*, 2005]. We inverted both the travel-time picks and the differential travel times for events with 1) epicentral distances of less than 200 km, and 2) inter-event distances smaller than 5 km. Because the seismic waves propagate similar ray paths between event and station, the differential time can be inverted as a function of the spatial offset between the events. As a result, the double-difference technique can relocate the relative earthquake locations more precisely (Figure 1).

[5] We perform cross correlation for both P and S phases from 780 events to derive 26978 arrival times from 692 events that show similar waveforms. We use differential travel time only if its correlation coherency, used to measure the similarity between the waveforms, is greater than 0.6. Overall the P waveforms show higher coherency than the S waveforms. We compare the consistency between differential times derived from P and S of the same waveform pair for the whole data set. ($P_{\text{differential time}} - S_{\text{differential time}}$) show a tight Gaussian distribution centered at zero with standard deviation less than 0.03 sec, corresponding to 150 m of location uncertainty using a P velocity of 5 km/sec The remaining 88 events, about 11% of the total events in the catalog, do not have good waveform correlations. To make our catalog more complete and to ensure accurate absolute hypocenters, we then included differential times derived from phase picks of the SCSN catalog. As a result, 55 more events were relocated. In the end, 747 out of 780 events occurring between 2003/1/1 and 2003/4/1 were relocated. Waveform-correlation gives moment centroid location while phase-pick differential times gives hypocenter. As a result, the inverted aftershock locations are more robust than that of the mainshock due to the shorter separation between the centroid and hypocenter for the aftershocks.

3. Relocated Seismicity

[6] The relocated aftershocks illuminate the mainshock rupture trend as well as several other cross-cutting trends

[1]Institute of Earth Sciences, Academia Sinica, Taipei, Taiwan.
[2]Formerly at Seismological Laboratory, California Institute of Technology, Pasadena, California, USA.
[3]Seismological Laboratory, California Institute of Technology, Pasadena, California, USA.

0094-8276/06/2005GL025033

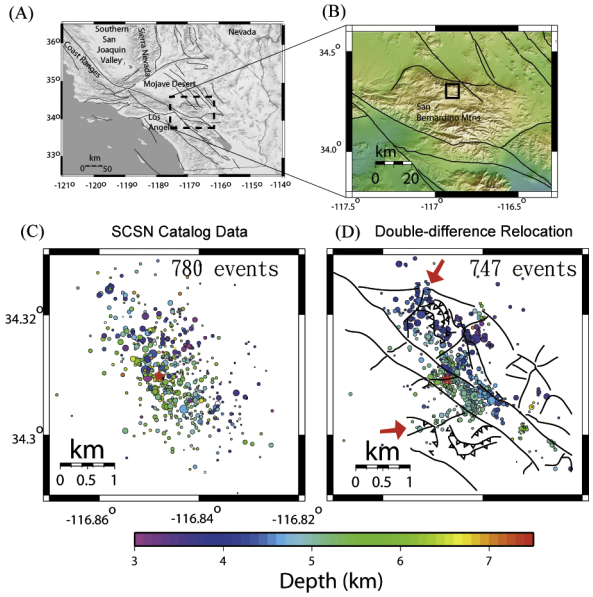

Figure 1. (a) Location of San Bernardino Mountains. (b) Location of the 2003 Big Bear Sequence. For comparison, we have plotted the seismicity using the following catalogs: (c) SCSN catalog and (d) from this study. The size of the circle is proportional to the magnitude of the earthquake. Color code shows the focal depth. The red star is the mainshock. We found good correlation between the double-difference relocated hypocenters and a published geologic map [*Sadler*, 1982] in this region. The 2 red arrows depict the 2 subvertical aftershock clusters which are perpendicular to the NW-SE trending mainshock fault.

(Figure 1). In cross section, the hypocenter of the mainshock is located within a 2.5 km by 1.8 km region devoid of aftershocks. In turn, this aftershock gap is surrounded by dense aftershock clusters on the mainshock fault, which dips slightly to the SW. The distribution of the aftershocks is consistent with regional fault mapping that reveals numerous fault traces cross-cutting each other at high angles [*Sadler*, 1982]. Only a subset of the known fault traces near the mainshock fault were activated during this sequence. From more than 100 sensitivity tests using different initial earthquake locations and different parameters for inversions, we found that the cross-fault aftershock pattern is a robust feature not controlled by the absolute locations for the aftershocks. The absolute locations as a whole can shift around by hundreds of meters as demonstrated in the sensitivity tests, depending on choice of damping parameters for the inversion and initial earthquake locations.

4. Style of Faulting

[7] We determined first motion focal mechanisms of these events using FPFIT program [*Reasenberg and Oppenheimer*, 1985]. The derived mechanisms exhibited mostly strike-slip and some thrust and normal focal mechanisms. Allowing for a 30° uncertainty in the cataloged strike, dip and rake values about 75% of the focal mechanisms are in good agreement with the vertical and sub-vertical fault planes illuminated by the relocated aftershocks.

[8] For moment tensor inversions of some Mw > 3.8 events, we integrated SCSN broadband waveforms to displacement and filtered between 0.02 and 0.05 Hz before downsampling from 100 to 1 sample per second. Each waveform trace is 100 s long to includes the complete waveforms. We have derived a preferred 1D velocity model (Table S1[1]) that gives the best travel time fits and waveform fits between observed and synthetic waveforms from forward modeling. We then used the procedure of *Dreger* [2003] to invert for moment tensors. Variance reductions, defined as 1 minus the standard deviation between the observed and synthetic waveforms. The variance reduction for the mainshock is above 75% for three-component waveforms from seven. Overall the waveform fits are excellent (Figure 2). The moment tensor for the mainshock has strike, dip, and rake of 136°, 71°, and −172°, respectively. Most of the larger aftershocks exhibit very similar strike-slip mechanisms but one aftershock exhibits an almost pure thrust mechanism (see Figure 3a and auxiliary material).

5. Slip Model and Static Stress Perturbation

[9] Because a detailed finite slip model for the Mw5.0 mainshock cannot be accurately determined, we approximate the mainshock rupture with a simple slip model, to see if it can explain the spatial distribution of aftershocks. We assume that the 2 km by 1.2 km region devoid of aftershocks on the mainshock fault plane represents the spatial extent of the mainshock slip model, Based on the moment released derived from the moment tensor inversion, we used an average slip of 0.26 m.

[10] We use this finite fault model to determine the Coulomb Failure Stress (CFS) perturbation caused by the mainshock based on the method of *Toda et al.* [2002]. To avoid stress singularities, we tapered the slip along the edges of the slip model to 0.026 m while conserving the total moment release. After tapering, the slip model produced a smoother butterfly pattern and wider CFS increase zone near the mainshock fault. We used an average north-south trending regional stress direction from *Hauksson* [1994] and calculated CFS changes using several receiver fault orientations. Because the overall patterns are similar, we show only the results from the optimal fault orientation (Figure 3). The CFS model exhibits 4 extensional lobes, where two are perpendicular to the mainshock fault and correlate with the relocated aftershocks clusters.

6. Discussion

[11] The complex geometrical distribution of the aftershocks is smaller in overall size but of similar complexity to what is often observed for much larger mainshocks such as Landers, Hector Mine, and Northridge earthquakes [e.g., *Hauksson et al.*, 2002]. We also found that an Mw5 earthquake can produce complex aftershock focal mechanisms. Several smaller aftershocks exhibited a large component of dip-slip movement and at least one large aftershock (M = 4.3) had a well-constrained pure thrust mechanism (Figure 3). The locations of these dip-slip events

[1]Auxiliary material is available at ftp://ftp.agu.org/apend/gl/2005gl025033.

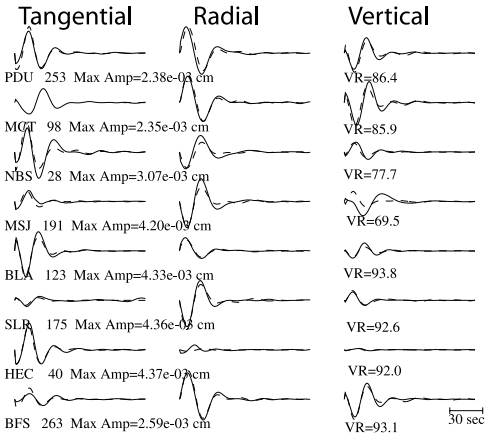

Figure 2. Waveform fits of the mainshock moment tensor inversions. The solid lines are the observed waveforms and the dashed lines are the synthetics. All waveforms are displacements filtered between 0.02 and 0.05 Hz. The texts under each three-component waveforms show the station name, epicentral distance in km, maximum amplitude of all three components in cm, and variance reduction in %. The focal mechanisms and the event locations are shown in Figure 3.

are less well-constrained because these aftershocks have waveforms that differ substantially from the neighboring strike-slip events. As a result, some of these events were not relocated using the time difference from waveform cross correlation. However, these events were relocated when we included the phase picks in the double-difference inversion. Most of these thrust faulting events were within the shadow zone for strike-slip receiver faults and the advanced zone for dip-slip receiver faults.

[12] Previously, the 60° conjugate fault model has been used to successfully predict active deformation style in other regions. For example, *Hauksson et al.* [2002] relocated the Hector Mine earthquake sequence and found the aftershock locations depict a typical 60° conjugate fault pattern that is consistent with the regional maximum horizontal stress direction. However, for the 2003 Big Bear sequence, both the derived orthogonal aftershock clusters and mapped geologic structures contradict the 60° conjugate fault model. The possible mechanisms for perpendicular aftershock clusters include faults with very low normal stress or friction [cf. *Twiss and Moores*, 1992]. Also, the Big Bear mainshock triggered mostly the faults in the extensional lobes, suggesting other triggering mechanisms related to radiation pattern of the mainshock are also important.

[13] The qualitative correlation between relocated anti-symmetric aftershock patterns and CFS changes argues that static stress perturbation from an Mw5.0 mainshock can be among the factors that controlled the occurrence of the fault-perpendicular aftershock clusters. Dynamic triggering can also be important. But it is hard to interpret why dynamic triggering did not trigger more faults in the CFS compressional lobes. The aftershock clusters are mostly located in the extensional region induced from the mainshock faulting, or behind the slip direction of the mainshock on both sides, thus forming the anti-symmetric pattern similar to that predicted from Griffith crack theory (Figure 3b). For pure strike-slip on a rectangular slip model on a vertical fault, the increased CFS regions define two major vertical seismicity zones located in the extensional quadrants. However, if there is a dip-slip component, there will be 2 more additional sub-horizontal seismicity zones at the top and bottom of the slip model. The deeper, and shallower sub-horizontal aftershock seismicity zones will be in the regions that moved up, and down, respectively, i.e., also in the extensional quadrants. We can also apply a similar approach to dip-slip faults, as long as the slip has relatively uniform direction and the slip patch is almost rectangular.

7. Conclusions

[14] We systematically studied several aspects of the 2003 Big Bear, California Sequence, including first motion inversion, complete waveform moment tensor inversion, aftershock relocation, and theoretical coulomb failure stress analyses. Previously it was difficult to study an Mw5 earthquake sequence in such details due to the uncertainties on aftershock locations and mainshock source parameters. The relocated aftershocks depict multiple fault traces, some of them perpendicular to the mainshock fault plane. The aftershocks show diverse focal mechanisms, based on moment tensor inversion and first motion mechanisms. We infer that the perpendicular seismicity was at least partially activated by the static stress transfer from the

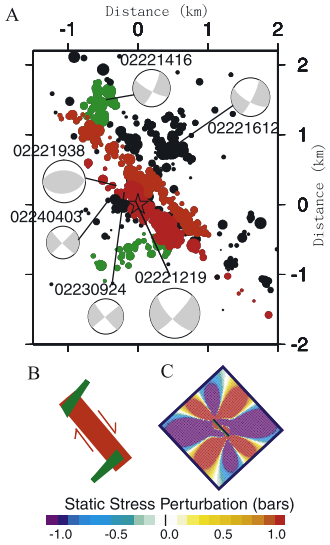

Figure 3. (a) Relocated hypo-DD hypocenters and examples of focal mechanisms derived from complete waveform moment tensor inversion and first motion grid-search. Red dots are interpreted as events on the mainshock fault system. Green dots are 2 sub-vertical aftershock clusters that are perpendicular to the aftershocks along the mainshock fault plane. The star denotes the mainshock location. The numbers above each beach ball are the month, day, hour, and minute of the event origin time. (b) A cartoon showing the spatial relation between the aftershocks along the mainshock rupture in red and the perpendicular aftershock clusters in green. (c) A schematic model showing how the right-lateral strike-slip mainshock generates an increase in stresses in the extensional lobes where we expect aftershocks.

mainshock. Other mechanisms such as weak fault and dynamic stress triggering might also be important Our rectangular slip model predicts that there will be two or four such perpendicular aftershock clusters if the slip is parallel or oblique to the slip model boundaries, respectively. This prediction can be tested for future mainshocks as more high resolution seismic catalogs, moment tensor catalogs, and finite fault solutions become available.

[15] **Acknowledgments.** We thank Debi Kilb for reviewing the manuscript. This study is partially supported by NEHRP/USGS Grant 04HQGR0052 and by SCEC, which is funded by NSF Cooperative Agreement EAR-0106924 and USGS Cooperative Agreement 02HQAG0008; SCEC contribution number 959. Additional supports came from National Science Council of Taiwan (NSC 94-2119-M-001, IESAS1113). Contribution number 9136, Division of Geological and Planetary Sciences, California Institute of Technology, Pasadena.

References

Dreger, D. S. (2003), TDMT_INV: Time Domain Seismic Moment Tensor INVersion, in *International Handbook of Earthquake and Engineering Seismology*, *Part B*, *Int. Geophys. Ser.*, vol. 81, p. 1627, Elsevier, New York.

Hauksson, E. (1994), State of stress from focal mechanisms before and after the 1992 Landers earthquake sequence, *Bull. Seismol. Soc. Am.*, *84*, 917–934.

Hauksson, E., and P. Shearer (2005), Southern California hypocenter relocation with waveform cross-correlation: part 1, Results using the double-difference method, *Bull. Seismol. Soc. Am.*, *95*, 896–903.

Hauksson, E., L. Jones, and K. Hutton (2002), The 1999 M_w 7.1 Hector Mine, California, earthquake sequence: Complex conjugate strike-slip faulting, *Bull. Seismol. Soc. Am.*, *92*, 1154–1170.

Kilb, D., and A. M. Rubin (2002), Implications of diverse fault orientations imaged in relocated aftershocksof the Mount Lewis, M_L5.7, California, earthquake, *J. Geophys. Res.*, *107*(B11), 2294, doi:10.1029/2001JB000149.

Reasenberg, P., and D. Oppenheimer (1985), FPFIT, FPPLOT and FPPAGE: FORTRAN computer programs for calculating and displaying earthquake fault-plane solutions, *U.S. Geol. Surv. Open File Rep.*, *85-739*, 109 pp.

Sadler, P. (1982), Geology of the northeast San Bernardino Mountains, San Bernardino County, California: Big Bear City Quad, *CDMG OFR 82–18*(D), Calif. Geol. Surv., Sacramento.

Toda, S., R. Stein, and T. Sagiya (2002), Evidence from the 2000 Izu Islands swarm that seismicity is governed by stressing rate, *Nature*, *419*, 58–61.

Townend, J., and M. Zoback (2001), Implications of earthquake focal mechanisms for the frictional strength of the San Andreas fault system, *Geol. Soc. Spec. Publ.*, *186*, 13–21.

Twiss, R. J., and E. M. Moores (1992), *Structural Geology*, 532 pp., W. H. Freeman, New York.

Waldhauser, F., and W. Ellsworth (2000), A double-difference earthquake location algorithm: Method and application to the northern Hayward Fault, California, *Bull. Seismol. Soc. Am.*, *90*, 1353–1368.

W.-C. Chi, Institute of Earth Sciences, Academia Sinica, 128 Academia Road, Sec. 2, Taipei, Taiwan. (chi@earth.sinica.edu.tw)

E. Hauksson, Seismological Laboratory, California Institute of Technology, 1200 E. California Blvd., MS 252-21, Pasadena, CA 91125–2100, USA.